Composition of high current arc plasma in Ar-H_2 mixture at moderate pressures

S Avtaeva[2], V Gorokhovsky[1], A Obrusnik[3], Z Zembower[1]

[1]Vapor Technologies, Inc., Longmont, Colorado, USA
[2]Institute of Laser Physics, Novosibirsk, Russia
[3]Plasma Solve, Ltd., Brno, Czechia

E-mail: s_avtaeva@mail.ru

Abstract. Composition of the high current low pressure arc discharge in a large chamber (0.5 m in diameter) in Ar-H_2 mixtures was studied by optical emission spectroscopy methods and was modeled utilizing thermodynamic and fluid models. The dissociation degree of molecular hydrogen was estimated using $I_{H\alpha}/I_{H2}$ intensity ratio of H_α line and Q1(0–0) line of the H_2 Fulcher's α-system. In addition, atomic hydrogen density was estimated using optical actinometry method from intensity ratio $I_{H\alpha}/I_{ArI}$ of the H_α and ArI 750 nm lines. Moreover, the H_2 dissociation degree across the discharge tube was modeled using LTE calculation based on minimization of isobaric-isothermal potential of the closed thermodynamic system with the help of commercial software TERRA. Alternatively, hydrogen thermal dissociation was calculated in an axially-symmetrical one fluid, one temperature approximation using commercial software COMSOL FEM; the thermal dissociation model relies on solving an advection-diffusion-reaction (ADR) equation for atomic hydrogen that is produced by Ar or H_2 impact and is lost in three-body recombination. The results of the comparison of hydrogen dissociation degree across the arc column demonstrate reasonably good agreement both with experimental findings and between two modeling approaches.

1. Introduction

Hydrogen plasmas can be created in different ways, for example, in dc glow discharges, rf plasma, mw plasma, in a hollow cathode discharges, cascaded arc etc. and have a wide range of applications [1]. One of the applications is diamond films deposition. It has been found that high quality diamond films are grown in a hydrogen diluted plasma, and that the atomic hydrogen present in these plasmas is essential for getting high-quality films [2]. Argon additive to hydrogen can enhance hydrogen plasma characteristics as the energy of metastable argon states, forming at Ar atom collisions with electrons, can be transferred to hydrogen molecules and then it can initiate dissociation and ionization of H_2 molecules. The high density low pressure hydrogen arc plasma has been used in various applications such as lighting sources, PACVD processes, synthesis of nano-powders, thermionic energy conversion, and electric propulsion [3-5]. Modern technologies needs a large volume discharge technique to provide necessary productiveness and to treatment and manufacture of large details.

The aim of our research was study of H_2 dissociation in the large-volume high-density low-pressure Ar -H_2 arc discharge and finding conditions for high dissociation degree of molecular hydrogen. The dissociation degree of molecular hydrogen was estimated using $I_{H\alpha}/I_{H2}$ intensity ratio of H_α line and the Q1(0–0) line of the H_2 Fulcher's α-system. In addition, atomic hydrogen density was estimated using

optical actinometry method from intensity ratio $I_{H\alpha}/I_{ArI}$ of the H_α and ArI 750 nm lines. Moreover, the dissociation of hydrogen across the discharge tube was calculated with assumptions of H_2 thermal dissociation by two ways. One model relies on LTE calculation based on minimization of isobaric-isothermal potential of the closed thermodynamic system using the commercial software TERRA, another model solves an advection-diffusion-reaction equation for atomic hydrogen, that is produced by Ar or H_2 impact and is lost in three-body recombination, using the COMSOL FEM software. The experimental setup and OES technique is described in section 2, effects of discharge current, gas pressure and Ar fraction in Ar-H_2 mixtures on H_2 dissociation degree derived by OES technique are presented in section 3 and modeling results are shortly reported in section 4.

2. Experimental setup

The sketch of the experimental setup is presented in figure1. The low-pressure discharge in a large chamber (approximately 0.5 m in diameter) is ignited between stainless steal anode of 18 mm diameter and moderate stainless steal cathode assembly; the electrodes were disposed at 90° angle to each other at distance of 40 cm as it is shown in figure 1.

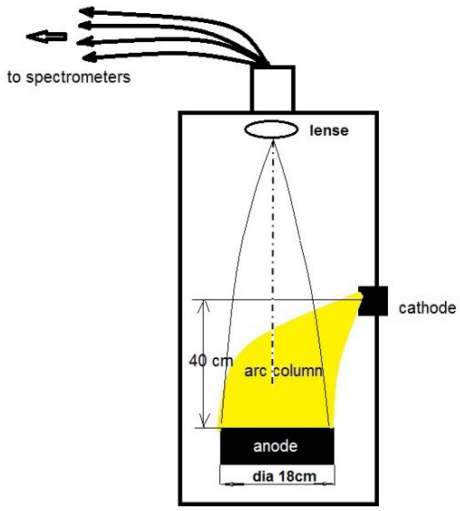

Figure 1. Experimental setup.

The discharge chamber was evacuated up to residual pressure of $2*10^{-5}$ Torr and then hydrogen and argon were injected up to 1-2.5 Torr. Gas consumption was measured using flow meters and were varied in a range of 640-3227 sccm. Ar/H_2 ratio was varied in the range of 0.05-0.2 by adjusting a ratio of gas flow rates. The discharge current was held at a level of 20-144 A and discharge voltage was varied in a range of 125-210 V.

The discharge possesses growing current-voltage characteristics, at the same time increase in discharge current at invariable Ar/H_2 ratio leads to rise in gas pressure even if gas flow rate is decreased (figure 2). The reasons for the effect are lifting gas temperature and dissociating H_2 in the discharge. Increase in pressure at invariable discharge current and Ar/H_2 ratio brings to rise in discharge voltage (figure 3a). Growth of Ar/H_2 ratio at unchanged pressure and discharge currents results in decreasing discharge voltage and needs diminishing gas flow rates (figure 3b).

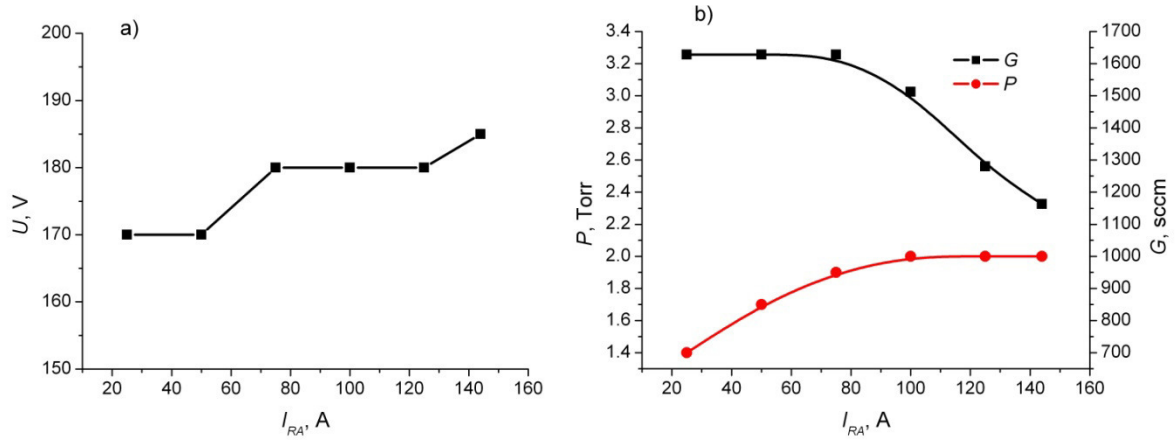

Figure 2. The discharge voltage (a), gas pressure and flow rate (b) as functions of anode current at P=1.4-2 Torr and Ar/H_2=0.14.

Radiation of the low-pressure arc was collected by a collimated lens, at that the arc column was generally aligned along the optical axis. The emission was then focused at the fiber optic cable divided in 4 channels to conduct plasma radiation toward a set of four Ocean Optics spectrometers HR-4000 with bandwidths of 199-428, 399-613, 600-799 and 800-972 nm, respectively. The devices (with gratings of 1200 L/mm) have optical resolutions of ~0.03 nm and have high sensitivity detectors. Relative sensitivity of the devices as a function of wavelength was calibrated using the DH-2000-CAL.

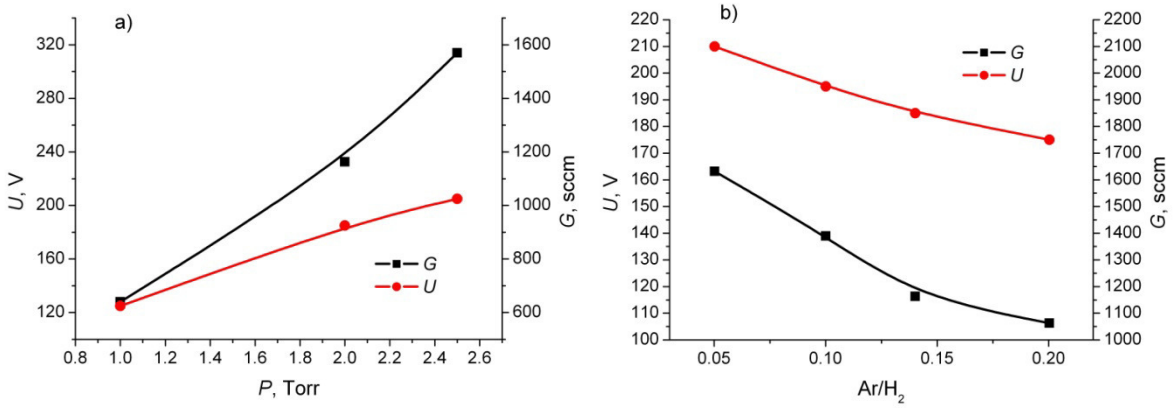

Figure 3. The discharge voltage and gas flow rate as functions of pressure (a) and gas composition (b).

3. H_2 dissociation degree measurements by OES technique

Figure 4 shows typical spectra of the arc discharge plasma in Ar-H_2 mixtures in the wavelength range of 400-800 nm. In spectra there are well visible H_β, H_γ and H_δ lines of atomic hydrogen together with lines of molecular hydrogen bands; there also are lines of argon atoms (ArI) in the wavelength range of 600-800 nm.

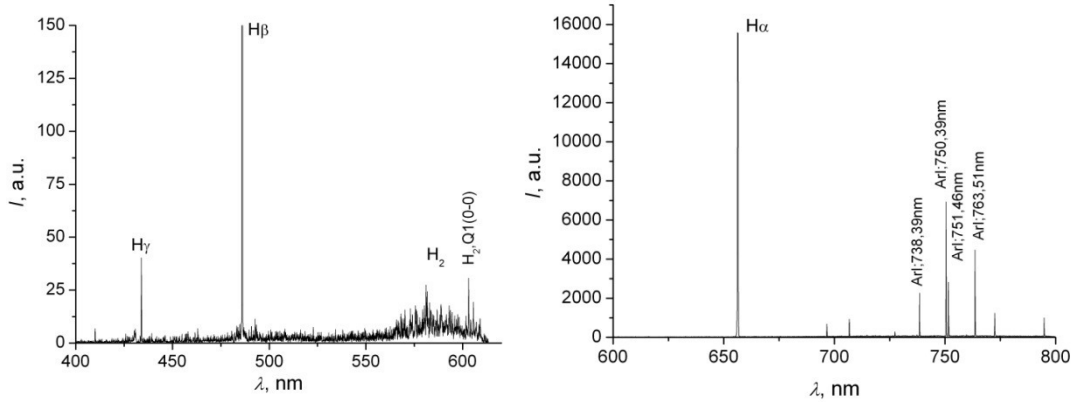

Figure 4. Spectrum of the arc discharge plasma in Ar-H_2 mixture in the wavelength range 400-800 nm at P=2 Torr, Ar/H_2=0.1, I=144 A, U=195 B.

The dissociation degree of molecular hydrogen was estimated using intensity ratio of H_α line and the Q1(0–0) line of the H_2 Fulcher's α-system $I_{H\alpha}/I_{H2F}$ [6]. In condition of coronal equilibrium, which is valid at low pressures, atomic and molecular hydrogen density ratio is related to intensity ratio of the Balmer-series Hα (6563 Å) line and the Q1(0–0) of the Fulcher-system of H_2 by the formula [6, 7]

$$\frac{N_H}{N_{H_2}} = \frac{I_{H_\alpha}}{I_{H_2F}} \cdot \frac{\lambda_{H_\alpha}}{\lambda_{H_F}} \frac{(f'_{rot}(k=1)/Q_{rot}) \cdot q_{v^0v'} \sigma_{em}^{(0-0)} q_{v'v''}}{\sigma_{\max}^{H(n=3)} A_{H_\alpha} \tau_{n=3}^{H}} \cdot \frac{1}{(1+C_{thr}(\varepsilon))}, \quad (1)$$

where N_H and N_{H2} are densities of H and H_2; $I_{H\alpha}$, I_{H2F}, $\lambda_{H\alpha}$, λ_{H2F} are the relative intensities and wavelengths of the H_α Balmer series and the Q1(0–0) of the H_2 Fulcher-system, respectively; $f'_{rot}(k=1)$ is the rotational distribution function of excited hydrogen molecules; $A_{H\alpha}$ is the H_α transition probability [8]; $\tau_{n=3}^{H}$ is the radiative lifetime of the H(n = 3) level [8]; $\sigma_{\max}^{H(n=3)}$ is the excitation cross section for the H(n = 3) level [9]; $\sigma_{em}^{(0-0)}$ is the excitation cross section for the Fulcher-system [10]; $q_{v^0v'}$, $q_{v'v''}$ are Franck-Condon factors, $R_{k'k''}$ is Hönl-London factor, and $C_{thr}(\varepsilon)$ is a correction factor, which takes into account the dependence of the cross sections on the electron energy [7, 10].

In addition, atomic hydrogen density was estimated using intensity ratio of H_α and ArI (750 nm) lines $I_{H\alpha}/I_{ArI}$ by the optical actinometry method. In condition of corona equilibrium, the density ratio of hydrogen and argon atoms N_H / N_{Ar} is related with the intensity ratio $I_{H\alpha}/I_{ArI}$ by the equation [11, 12]:

$$\frac{N_H}{N_{Ar}} = \frac{A_{ki}^{Ar} \nu_{ki}^{Ar} \sigma_{\max}^{Ar} f_{13.47eV} \tau_k^{Ar}}{A_{ki}^{H} \nu_{ki}^{H} \sigma_{\max}^{H} f_{12.09eV} \tau_k^{H}} \cdot \frac{I_{H\alpha}}{I_{ArI}}, \quad (2)$$

Here A, ν, $\sigma_{\max}$, τ, f are transition probabilities, frequencies, threshold cross sections, life times and the EEDF at threshold value, which values were obtained from [8, 9, 11] for hydrogen Hα and from [8, 11-13] for ArI (750 nm).

Intensities of the Balmer-series Hα line (656.3 nm), the Q1(0–0) line of the Fulcher-system of H_2 and ArI (750 nm) line in emission spectra of the Ar-H_2 discharge as functions of anode current, gas pressure and Ar/H_2 ratio are shown in figures 5a, 6a and 7a, correspondingly.

One can see, intensities of all three lines grow with anode current, but intensity of Hα line increases faster as compared with intensities of the H_2 and Ar lines (figure 5a). Rising gas pressure at unchanged ratio of Ar/H_2 leads to decreasing intensities of of the ArI and H_2 lines, but intensity of Hα line remains almost unchanged (figure 6a). When Ar fraction in Ar-H_2 mixture increases, the intensities of ArI and Hα lines rise, but intensity of the H_2 line (Q1(0–0), Fulcher-system) decreases (figure 7a).

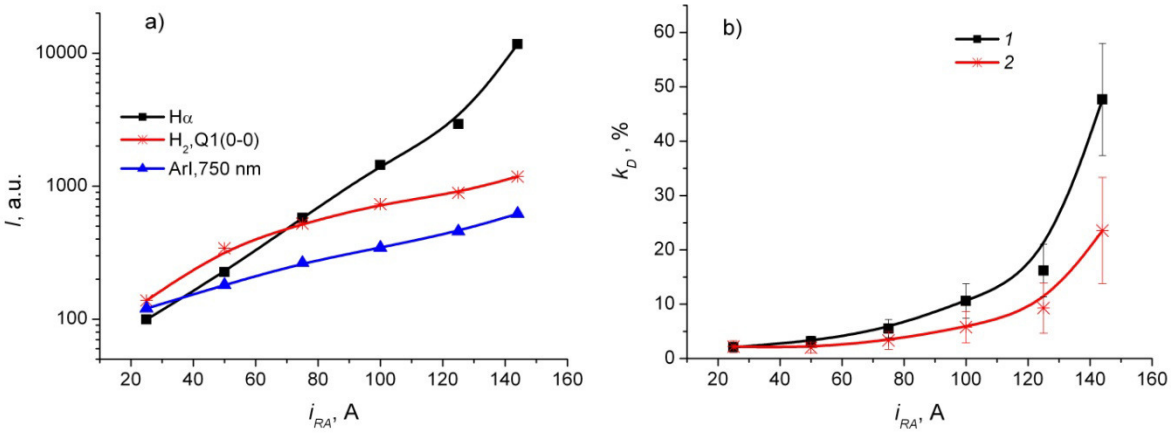

Figure 5. Intensities of the Hα 656.3 nm, the Q1(0–0) of the Fulcher-system of H_2 and ArI 750 nm (a) and H_2 dissociation degree derived from $I_{H\alpha}/I_{Ar}$ and $I_{H\alpha}/I_{H2Q1(0-0)}$ (b) as functions of the anode current; P=1.4-2 Torr, Ar/H_2=0.14, U=170-180 V.

Both intensity ratios $I_{H\alpha}/I_{Ar}$ and $I_{H\alpha}/I_{H2}$ increase with discharge current and gas pressure, that is result of the H_2 dissociation degree rise with the discharge current and gas pressure (figures 5b, 6b). Increasing Ar fraction in Ar-H_2 mixtures (rise in Ar/H_2 ratio) also results in growth of the hydrogen dissociation degree (figure 7b).

Increasing H_2 dissociation degree with anode current points at role of electrons in hydrogen dissociation; electrons can initiate the dissociation directly at electron collisions with hydrogen molecules as well as indirectly via Ar metastable state excitation and gas heating. Increase in pressure results in electron density decreasing and so intensities of the H_2 and Ar lines decreases (figure 6a), but rate of hydrogen dissociation grows due to increasing the thermal dissociation rate with increase in the thermal collisions frequency. Rise in hydrogen dissociation with increasing Ar/H_2 ratio can be related to contribution of Ar metastable states in H_2 dissociation.

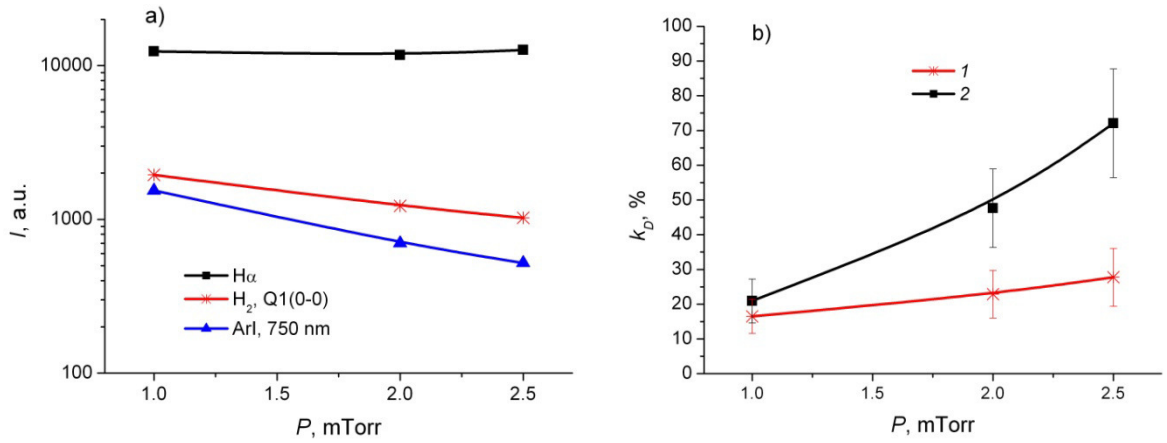

Figure 6. Intensities of the Hα 656.3 nm, the Q1(0–0) of the Fulcher-system of H_2 and ArI 750 nm (a) and H_2 dissociation degree derived from $I_{H\alpha}/I_{Ar}$ and $I_{H\alpha}/I_{H2Q1(0-0)}$ (b) as functions of gas pressure; I=144A, Ar/H_2=0.14, U=125-205 V.

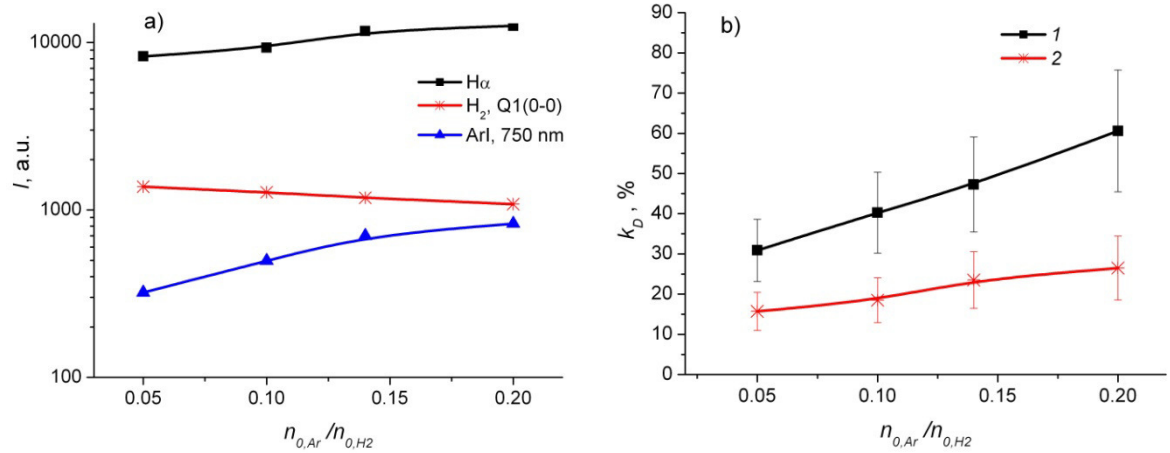

Figure 7. Intensities of the Hα 656.3 nm, the Q1(0–0) of the Fulcher-system of H_2 and ArI 750 nm (a) and H_2 dissociation degree derived from $I_{H\alpha}/I_{Ar}$ and $I_{H\alpha}/I_{H2Q1(0-0)}$ (b) as functions of Ar/H_2 ratio; P=2 Torr, I=144A, U=175-210 V.

As one can see, H_2 dissociation degree calculated using $I_{H\alpha}/I_{Ar}$ ratio is higher that calculated by $I_{H\alpha}/I_{H2}$. At the same time, all dependences of the H_2 dissociation degree k_D on discharge conditions

(anode current, gas pressure and Ar-H_2 mixture composition) derived using $I_{H\alpha}/I_{Ar}$ and $I_{H\alpha}/I_{H2}$ intensity ratios are similar. The similar dependences conform a possibility to use both intensity ratios $I_{H\alpha}/I_{Ar}$ and $I_{H\alpha}/I_{H2}$ to control H_2 dissociation degree, the ratios are very sensitive to change in N_H/N_{H2} ratio and less sensitive to changing temperatures (T_e, T_{vib}, T_{rot}, T_g). At the same time accurate measurements of the hydrogen k_D using $I_{H\alpha}/I_{Ar}$ or $I_{H\alpha}/I_{H2}$ intensity ratios presents some difficulties because for precise calculation of the k_D it is necessary to know the temperatures (or distribution functions).

4. Modeling H_2 dissociation in the low-pressure arc discharge

The low pressure arc plasma was modeled in an axially-symmetrical one fluid, one temperature approximation using commercial software COMSOL FEM. The thermal dissociation model relies on solving an advection-diffusion-reaction (ADR) equation for atomic hydrogen that is produced by Ar or H_2 impact and is lost in three-body recombination. Hydrogen thermal dissociation was calculated via 3-body reactions: 2H + M <=> H_2 + M, where M=H_2, H or Ar, and the reaction rates were taken from [14]. The transport properties of Ar-H_2 thermal plasma were taken from [15].

Alternatively, the dissociation of the hydrogen across the discharge tube was calculated by thermal dissociation and via LTE calculation based on minimization of isobaric-isothermal potential of the closed thermodynamic system similar to the approach presented in [16 17], using commercial software TERRA, developed by Prof. B.G. Trusov (the latest version of the former software ASTRA).

In the ADR approach, the less number of reactions affecting hydrogen dissociation are included compare to LTE calculation, while diffusion losses to the chamber walls are taken into account, which is expected to produce less nascent hydrogen than in LTE conditions. On the other hand, LTE gives the dissociation degree coupled to the local temperature while the ADR approach gives broad spreading of the nascent hydrogen cloud toward the cooler area of the discharge. The results of the comparison of hydrogen dissociation degree across the arc column shown in figure 8 demonstrate reasonably good agreement both with experimental findings and between two modeling approaches.

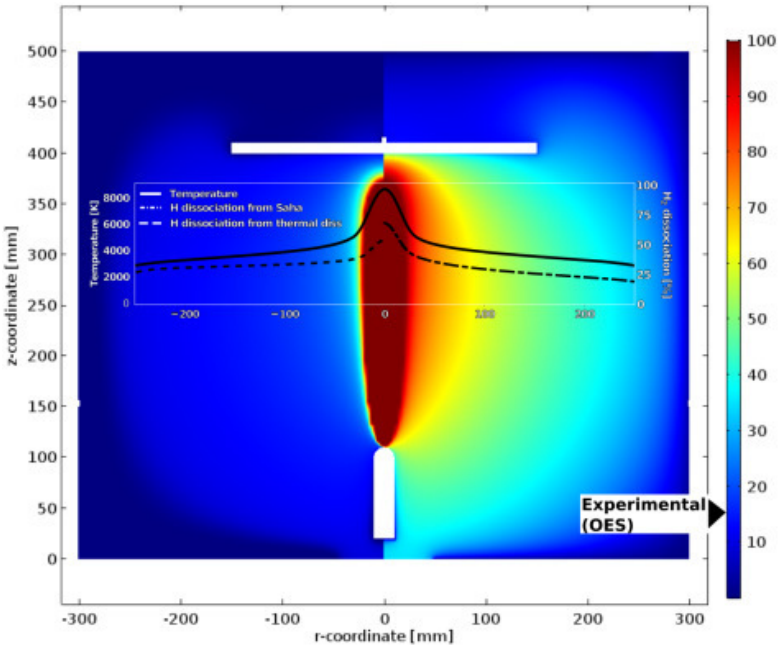

Figure 8. Comparison of the modeling distributions of H_2 dissociation degree across the column of 10%Ar-90%H2 arc obtained from Saha equilibrium (left) and advection-diffusion-reaction equation (right) at P=2 mTorr and I=150 A.

5. Conclusions

The composition of high current low pressure arc discharge in a large chamber (approximately 0.5 m in diameter) in an Ar-H_2 mixture was studied by optical emission spectroscopy methods. The dissociation degree of molecular hydrogen was estimated using $I_{H\alpha}/I_{H2}$ intensity ratio of H_α line and Q1 rotational line of the (0–0) vibrational band of the molecular hydrogen Fulcher's α-system, showing the dissociation degree of hydrogen in the arc plasma is about 15-20% at discharge current of about 150 A. In addition, atomic hydrogen density was estimated using optical actinometry method from intensity ratio $I_{H\alpha}/I_{ArI}$ of the H_α and ArI 750 nm lines, displaying hydrogen dissociation degree in 2-3 times higher than obtained from $I_{H\alpha}/I_{H2}$ ratio. Both intensity ratios show simile dependences of H_2 dissociation degree on discharge parameters, namely, discharge current, gas pressure and Ar fraction in Ar-H_2 mixtures. Therefore, both intensity ratios $I_{H\alpha}/I_{Ar}$ and $I_{H\alpha}/I_{H2}$ can be used to control H_2 dissociation degree, the ratios are very sensitive to change in N_H/N_{H2} ratio and less sensitive to changing temperatures (T_e, T_{vib}, T_{rot}, T_g). At the same time the precise (accurate) measurement of hydrogen k_D using $I_{H\alpha}/I_{Ar}$ or $I_{H\alpha}/I_{H2}$ intensity ratios is difficult because we should know all temperatures at least and as maximum all distribution functions. There is good reason to believe that using $I_{H\alpha}/I_{H2}$ ratio for the Ar-H_2 arc allows to obtain more correct values of H_2 dissociation degree compared with utilizing $I_{H\alpha}/I_{Ar}$ ratio.

In addition, the low pressure arc plasma was modeled in an axially-symmetrical one fluid, one temperature approximation using commercial software COMSOL FEM, where dissociation of the hydrogen across the discharge tube was calculated by thermal dissociation model. The model relies on solving an advection-diffusion-reaction (ADR) equation for atomic hydrogen that is produced by Ar or H_2 impact and is lost in three-body recombination. Moreover, the H_2 dissociation was obtained via LTE calculation based on minimization of isobaric-isothermal potential of the closed thermodynamic system. The results of the comparison of hydrogen dissociation degree across the arc column demonstrate reasonably good agreement both with experimental findings and between two modeling approaches.

References

[1] Qing Z, Otorbaev D K, Brussaard G J H, van de Sanden M C M, and Schram D C 1996 *J. Appl. Phys.* **80** 1312.

[2] *Diamond Films '94* 1994 ed. by P K Bachmann, I M Buckley-Golder, J T Glass, and M Kamo (Elsevier, Amsterdam).

[3] Lavrov B P and Melnikov A S, Käning M and Röpcke J 1999 *Phys. Rev. E* **59** 3526.

[4] Böhrk H and Auweter-Kurtz M 2009 *Progress in Propulsion Physics* **1** 381.

[5] Rasor N S 1991 *IEEE Trans. Plasma Sci.* **19** 1191.

[6] Avtaeva S V and Lapochkina T M 2007 *Plasma Physics Reports* **33** 774.

[7] Van de Graaf M J 1994 *A new hydrogen particle source* PhD Thesis (Technical University Eindhoven, Eindhoven).

[8] Gruzdev P F 1990 *Transition Probabilities and Radiative Lifetimes of Atomic and Ionic Levels* (Énergoatomizdat, Moscow).

[9] Calloway J 1988 Phys. Rev. A. **37** 3692.

[10] Möhlmann G R, de Heer F J 1976 *Chem. Phys. Lett.* **42** 240.

[11] Avtaeva S V, Mamytbekov M Z, Otorbaev D K 1997 *J. Phys. D: Appl. Phys.* **30** 3000.

[12] Galtsev V E, Ivanov Yu A, Slovetskii D I, Rytova N M, Timakin V N 1983 *High Energy Chemistry* **17** (2) 164.

[13] Chutjon A, Cartwright D C 1981 *Phys. Rev. A.* **23** 2178.

[14] Gerasimov G Ya and Shatalov O P 2013 Journal of Engineering Physics and Thermophysics **86** 987.

[15] Murphy A B 2000 *Plasma Chem. Plasma Proc.* **20** 279.

[16] Gorokhovsky V 2005 Surface and Coatings Technology **194** 344.

[17] Vatolin N A, Moiseev G K, Trusov B G 1994 *Thermodynamic Modeling of High Temperature Inorganic Systems* (Metallurgy, Moscow).